INTERNATIONAL JOURNAL OF MULTIDISCIPLINARY FUTURISTIC DEVELOPMENT

Conceptual Model for Regeneration of Biodiesel from Agricultural Feedstock and Waste Materials

Augustine Tochukwu Ekechi [1*], Semiu Temidayo Fasasi [2]
[1] Borax Energy Services Limited, Port Harcourt, Nigeria
[2] Independent Researcher, Nigeria

* Corresponding Author: **Augustine Tochukwu Ekechi**

Article Info

P-ISSN: 3051-3618
E-ISSN: 3051-3626
Volume: 01
Issue: 02
July – December 2020
Received: 05-09-2020
Accepted: 07-10-2020
Published: 04-11-2020
Page No: 154-169

Abstract
This paper proposes a conceptual model for regenerating biodiesel from agricultural feedstock and waste materials, integrating circular-economy design with process intensification and digital optimization. The model comprises three layers: (i) feedstock valorization, (ii) catalytic conversion and purification, and (iii) data-driven control and sustainability assessment. In layer one, lipid-rich crops, used cooking oils, animal fats, and lignocellulosic residues are screened via multi-criteria decision analysis to balance cost, carbon intensity, free fatty acid content, and regional availability. Pre-treatment steps degumming, drying, deacidification, and particle-size reduction standardize variable inputs and reduce downstream fouling. Layer two specifies flexible transesterification and esterification trains employing bifunctional solid acid–base catalysts, reactive distillation, and ultrasound or microwave assistance to accelerate kinetics, limit soap formation, and shift equilibria. Membrane-assisted phase separation and deep eutectic solvent polishing minimize methanol loss and capture trace metals, water, and particulates. Closed-loop solvent recovery and glycerol upcycling into epoxides, biopolymers, or green hydrogen feed expand revenue and reduce waste liabilities. Layer three overlays a cyber-physical control architecture. Soft sensors estimate FFA, moisture, viscosity, and catalyst activity, hybrid models combine first-principles kinetics with machine-learning surrogates to optimize residence time, alcohol-to-oil ratio, temperature, and regeneration cycles. A dynamic life-cycle assessment quantifies carbon intensity, water stress, and eutrophication in near-real time, while techno-economic modules stress-test margins under feedstock price swings, carbon policies, and renewable-fuel credit markets. Governance and finance elements align with ISO 14040/44 and ISO 20400, enabling sustainability-linked procurement, traceable chains-of-custody, and community co-ownership. A resilience submodule introduces scenario planning for feedstock shocks, catalyst fouling, and policy shifts, using stochastic optimization to sustain ≥95% uptime. Deployment favors hub-and-spoke micro-refineries proximate to cluster farms and urban waste streams, reducing transport emissions and creating rural and peri-urban jobs. The model advances the field by translating dispersed methods into a reproducible blueprint adaptable to local agronomy and waste baselines. It also defines measurable key performance indicators conversion efficiency, energy return on energy invested, carbon intensity, and social co-benefits to drive continuous improvement and transparent reporting. Validation will pair pilots with sensitivity analyses and uncertainty quantification to establish replicability, bankability, and policy relevance. Results will inform standards, incentives, and equitable market participation.

DOI: https://doi.org/10.54660/IJMFD.2020.1.2.154-169

Keywords: Biodiesel Regeneration, Agricultural Feedstock, Waste Oils, Transesterification, Esterification, Solid Catalysts, Reactive Distillation, Membrane Separation, Deep Eutectic Solvents, Cyber-Physical Systems, Life-Cycle Assessment, Techno-Economic Analysis, Circular Economy, Micro-Refineries, Glycerol Upcycling.

1. Introduction

The transition to low-carbon fuels is constrained by inconsistent feedstock quality, elevated free fatty acid (FFA) levels, and the logistical and environmental burdens of waste handling across agricultural and urban streams. Variability in moisture, contaminants, and lipid composition undermines process stability, while high FFA promotes soap formation, catalyst deactivation, and off-spec biodiesel that struggles to meet ASTM/EN standards.

Simultaneously, dispersed supplies of used cooking oils, animal fats, and lignocellulosic residues impose collection, storage, and pretreatment penalties that erode margins and heighten operational risk. In response, this study proposes a modular, circular model for biodiesel regeneration that integrates feedstock valorization, flexible conversion pathways, and closed-loop separation and solvent recovery within a cyber-physical control layer (Al-Yafei, 2018, Parks & Pack, 2013).

The model is designed to standardize heterogeneous inputs through targeted pretreatment, route low- and high-FFA streams to tailored esterification/transesterification trains using solid catalysts and process-intensified operations, and recover methanol and co-products while minimizing waste liabilities via glycerol upcycling. Its scope spans feedstock mapping and traceability, pretreatment and inhibitor removal, catalytic conversion with in-situ quality monitoring, membrane-/reactive-separation hybrids, and data-driven optimization that couples first-principles kinetics with machine-learning surrogates.

Key contributions include a decision framework for adaptive routing under variable FFA and moisture, an operational blueprint for small, hub-and-spoke micro-refineries proximal to farms and urban waste streams, and a measurement architecture that links real-time soft sensors to sustainability accounting. Performance will be assessed against explicit key performance indicators conversion yield, carbon intensity per megajoule, energy return on energy invested (EROEI), and unit production cost supported by sensitivity and uncertainty analyses to guide scale-up, financing, and policy alignment (Hamilton, 2014, Udie, Bhattacharyya & Ozawa-Meida, 2018).

2. Methodology

The methodology integrates predictive analytics, thermodynamic/exergy thinking, and secure, auditable operations to regenerate biodiesel from heterogeneous agricultural and waste streams. First, feedstock prospecting and intake follow a multi-criteria decision analysis that scores used cooking oil, animal fats, oil crops, and lignocellulosic residues on free-fatty-acid and moisture levels, metals/soaps, seasonal availability, distance/logistics, and price volatility. A zero-trust, tokenized chain-of-custody tags each batch from source through processing, and stratified sampling with rapid spectroscopy establishes priors for routing. Incoming material is standardized via filtration (50–1 μm staged), thermal/flash drying to moisture targets <0.05–0.10 wt%, degumming with water/acid to remove phosphatides, and deacidification (adsorptive or mild esterification) to collapse FFA tails that would otherwise poison base catalysts. Inline analyzers (FFA via titration proxies, viscosity/density, dielectric/moisture) feed soft sensors that fuse lab and process signals; Bayesian data reconciliation flags outliers and assigns each lot to a conversion pathway with quantified confidence.

Two intensified conversion trains operate in parallel and merge downstream. Low-FFA streams undergo base-catalyzed transesterification on regenerable solid bases or bifunctional catalysts, optionally in reactive distillation to couple reaction and separation, with alcohol-to-oil ratio, temperature, and residence time continuously optimized. High-FFA streams first pass through acid-catalyzed esterification on solid acids (e.g., sulfated zirconia, heteropolyacids on supports) with ultrasound/microwave assistance to reduce mass-transfer limits; they then join the base train for completion. Both trains implement design-of-experiments start-up and move to model-predictive control once response surfaces are learned, holding ester content ≥96.5% while minimizing alcohol consumption, heat duty, and catalyst deactivation. Catalyst stewardship uses condition-based regeneration (calcine/solvent wash) triggered by activity soft sensors; a rolling-horizon optimizer arbitrates alcohol recycle, purge, and make-up.

Crude product passes to high-g centrifugation or membrane phase splitters sized from operability windows that balance throughput against emulsion risk; overhead methanol is recovered via energy-integrated distillation and returned to the trains. Polishing combines adsorbents and deep eutectic solvents to pull residual soaps, trace glycerin, and metals below ASTM D6751/EN 14214 limits; optional wash/dry skids are enabled when conductivity/soap monitors cross thresholds. Glycerol co-product is valorized along pre-qualified routes catalytic epoxidation, fermentation/biopolymer precursors, or reformer H_2 feed selected by a margin-ranking model that ingests local energy prices and offtake contracts. Waste-heat pinch analysis couples dryer, distillation, and building services; fouling/slagging risk is assessed with exergy and exergoenvironmental metrics adapted from gas-turbine optimization literature to keep specific CO_2-eq and water footprints within targets.

A cyber-physical layer closes the loop. First-principles mass/energy balances hybridized with machine learning create soft sensors for FFA, conversion, and fouling indices; MPC manipulates alcohol flow, temperature, recycle ratios, and phase-split conditions to meet quality at minimum energy while enforcing safety and operability constraints. A digital twin performs sensitivity and uncertainty analyses (Monte Carlo on feed quality, catalyst life, demand) and serves scenario planning for feedstock shocks. Multi-objective optimization (yield/CI/EROEI/OPEX/CAPEX, uptime ≥95%) uses ε-constraint or Pareto search; TEA and dynamic LCA calculate payback and LCFS/RIN revenue under price/credit ranges, and risk scoring from capital-structure literature sets prudent leverage for micro-refinery rollout. Governance mirrors zero-trust networking: role-based access, encrypted data paths, audit trails, and automated batch genealogy. HSE is embedded through hazard identification (alcohol vapor, pressure, hot utilities), engineered safeguards, and legal emissions/waste compliance tracking.

Deployment follows a hub-and-spoke architecture. Community-scale pre-treatment hubs near farms and urban waste streams densify and standardize feedstock; spokes feed modular conversion skids that can be reconfigured for seasonal chemistries. Route optimization minimizes haulage and queues; contracts incorporate service-level agreements for quality/volume with social-interaction incentives to stabilize supply networks. Continuous improvement runs A/B tests (e.g., catalyst grade, ultrasound energy, polishing recipes) with causal inference to attribute outcomes; SPC and reliability metrics separate common-cause variation from assignable causes and trigger kaizen. The methodology's backbone predictive routing, intensified dual-train conversion, tight separation/polishing, cyber-physical optimization, and auditable governance yields a scalable, resilient pathway to regenerate biodiesel from diverse wastes into on-spec product with verifiable carbon intensity reductions.

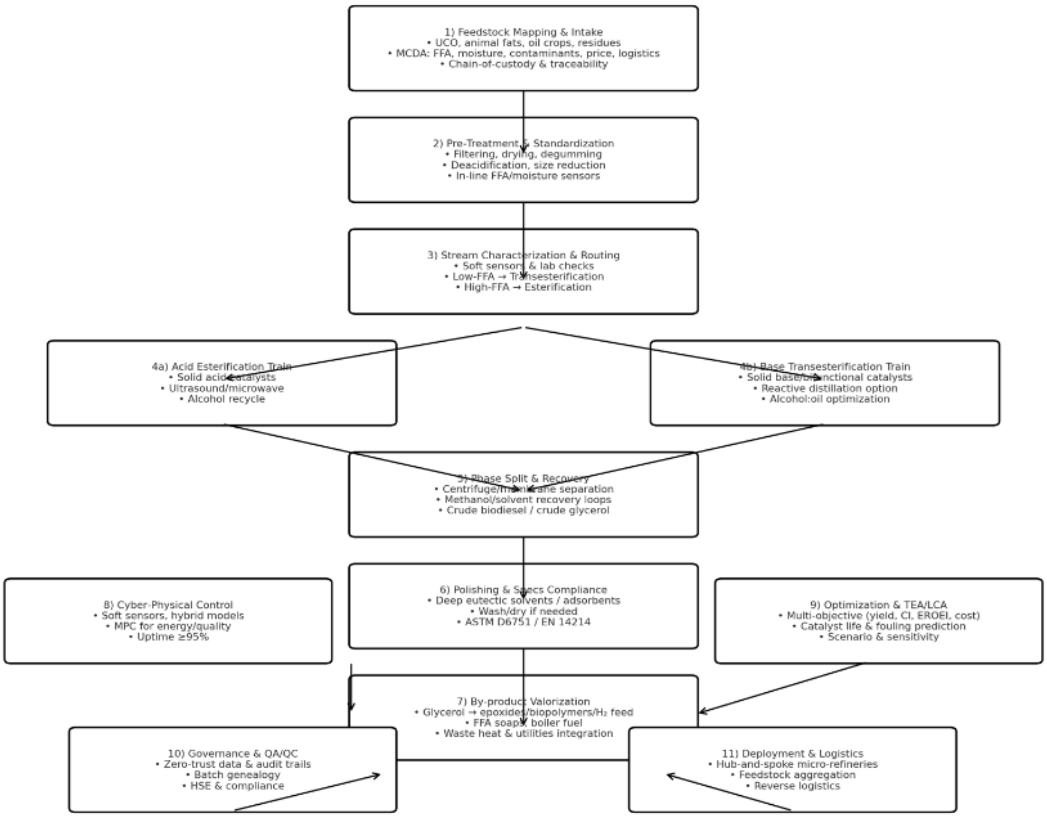

Fig 1: Flowchart of the study methodology

2.1. Feedstock Mapping & Selection

Feedstock mapping and selection is the pivotal first step in a conceptual model for regenerating biodiesel from agricultural feedstock and waste materials, because upstream variation dictates downstream chemistry, separation performance, plant uptime, and unit economics. The objective is to build an evidence-based inventory of feasible inputs, quantify their risks and opportunities, and allocate them to fit-for-purpose conversion routes while maintaining verifiable chain-of-custody across the supply network. Four source families define the accessible universe. Used cooking oil offers large urban volumes at low marginal cost but arrives heterogeneously, bearing water, soaps, bread crumbs, and polymerized triglycerides from repeated heating. Animal fats provide stable lipid content and favourable energy density, yet solidify at ambient temperatures and may contain proteins, salts, and moisture that complicate pretreatment and transport (Lu, *et al*., 2019, Nguyen, 2014). Oil crops supply predictable chemistry and scalable contracts but expose the operation to land-use debates and commodity price swings. Lignocellulosic residues straw, husks, pruning wastes, mill by-products, and energy grasses extend the feedstock base through thermochemical or biochemical upgrading to lipids or intermediates while imposing moisture and ash constraints that affect storage stability and reactor fouling.

Because no single stream dominates across regions or seasons, screening must be disciplined and transparent. A multi-criteria decision analysis ranks candidate on technical, environmental, social, and economic dimensions with explicit uncertainty. The core technical attributes are free fatty acid content, moisture, solids, polymerized fractions, and trace contaminants such as phosphorus, sulfur, alkali metals, and soaps that foul catalysts and membranes. High free fatty acid content accelerates saponification in base-catalyzed transesterification and therefore signals routing to acid esterification or solid acid catalysts before finishing. Moisture increases hydrolysis, dilutes alcohol, and raises energy demand during drying, so acceptance thresholds and price deductions are set accordingly. Phosphorus and metals promote catalyst poisoning and ash in glycerol, implying more aggressive adsorption or membrane polishing. For lignocellulosic pathways, cellulose–hemicellulose–lignin ratios, ash content, and alkali index influence char quality, bed agglomeration, and cleaning cycles, shaping pretreatment choices (Aljamel, 2010, Bidgoli, 2018).

Environmental and social criteria complement chemistry by addressing waste diversion, land stewardship, and community impacts. Used cooking oil typically earns high marks for displacing improper disposal; animal fats may be constrained by rendering regulations and odour controls; oil crops benefit from soil-health practices such as cover cropping and reduced tillage; lignocellulosic residues must respect soil organic carbon maintenance and erosion control so that removal rates do not degrade long-term productivity. Scores are combined with stakeholder weights derived from workshops with farmers, municipalities, and plant operators to produce auditable rankings and contingency plans (Cowie, *et al*., 2018, Lai, *et al*., 2011).

Economic criteria incorporate purchase price indexed to energy content, price volatility, seasonality of supply, and the full landed cost after collection, aggregation, storage, and pretreatment. Seasonality is characterized through historical production records and forward signals such as harvest calendars, restaurant density, slaughter schedules, and tourism cycles that sway food-service waste volumes. Logistics are modelled with travel-time and tonnage constraints, container availability, spillage rates, and heating needs for high-tallow streams. Storage risks oxidation,

microbial growth, and water settling are quantified as expected quality decay and remediated through filtration, inert blanketing, and first-in, first-out rotations. The decision model outputs a shortlist of primary and secondary feedstocks for each hub, paired with switch rules that trigger when weather, disease, market shocks, or policy changes shift availability or cost (Ahmadi & Dincer, 2011, Gimelli & Sannino, 2018).

Operationalizing the analysis requires geospatial mapping of sources, volumes, and quality attributes. Collection nodes restaurants, markets, smallholder farms, slaughterhouses, oil mills, and municipal transfer stations are digitized with coordinates, contact details, contractual status, and expected generation profiles. For used cooking oil, route planners cluster stops to balance payload, contamination risk, and pickup windows; standardized containers and tamper-evident seals reduce adulteration. For animal fats, coordination with cold-chain providers or jacketed tankers prevents solidification; receiving depots are equipped with heated lines and coarse strainers (Aref, 2012, Pathirathna, 2013). For oil crops, contracts specify moisture bands at delivery, acceptable impurity levels, and sampling protocols. For lignocellulosic residues, bale density, moisture, and tarp coverage are tracked to minimize mould and dry-matter loss, and removal rates are capped to protect soil cover and nutrient cycles. Figure 2 shows fermentation and gasification pathways to produce bioethanol and biodiesel from lignocellulosic biomass presented by Whalen, *et al*., 2017.

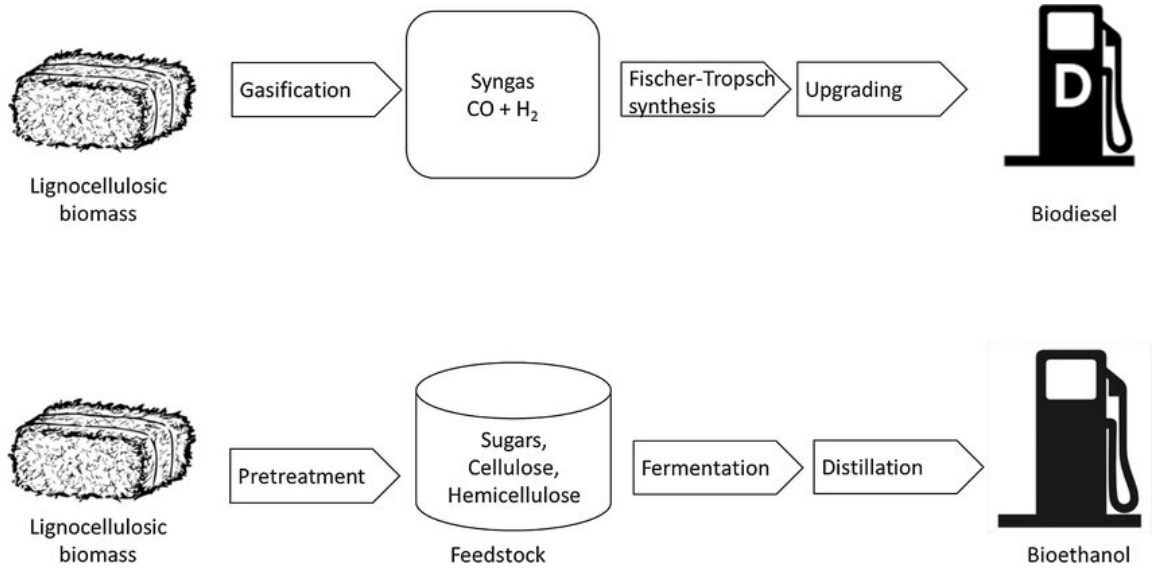

Fig 2: Fermentation and gasification pathways to produce bioethanol and biodiesel from lignocellulosic biomass (Whalen, *et al*., 2017).

Traceability and chain-of-custody are essential to prevent fraud, ensure safety, and substantiate sustainability claims. Each batch receives a unique digital identifier at first custody transfer, linked to source type, coordinates, time stamp, batch size, and preliminary quality tests. Transfers between collectors, aggregators, and the refinery are recorded as signed events with geotagged, time-stamped records, calibrated scales, and, where feasible, mass-flow meters to reconcile volumes. Documentation captures sanitation status of tanks, temperature at loading, and container condition. The traceability ledger integrates with sustainability accounting so that recycled-content claims and carbon-intensity calculations reflect actual provenance and processing conditions rather than generic defaults, and it provides the audit trail required by procurement policies and renewable-fuel credit programs (Majoumerd, *et al*., 2014, Yee, Milanović & Hughes, 2010).

To convert mapping into procurement, the program defines supplier tiers, pricing structures, and quality incentives that align external behaviour with internal process constraints. Contracts offer base prices within grade bands plus premiums for low-moisture, low-FFA loads and penalties for contaminants that elevate pretreatment cost. Rapid payment and reliable pickup schedules enhance supplier loyalty and reduce leakage to informal markets. Micro-generators are aggregated into hubs with shared storage, filtration, and simple testing kits; vendor scorecards, refreshed monthly, rank suppliers by on-time readiness, documentation completeness, and delivered quality, enabling preferential routing, contract renewals, and targeted training (Larsson, *et al*., 2014, Li, Zhang & Ying, 2018).

Because screening and selection evolve with weather, market dynamics, and learning, the model embeds feedback loops. Statistical process control charts monitor feedstock attributes over time; outliers trigger supplier coaching or reclassification. Bayesian updating refines prior distributions for FFA, moisture, and contamination rates, improving routing decisions between esterification and transesterification trains and informing stocking policies for adsorbents and membranes. Portfolio stress tests simulate diesel price shocks, rendering plant outages, droughts that limit crop residues, or regulation that redirects edible oils to food programs, ensuring the refinery can pivot among approved sources without breaching quality or cost limits. Figure 3 show simplified scheme for industrial biodiesel production from feedstocks with low FFA and water content presented by Moser, 2010.

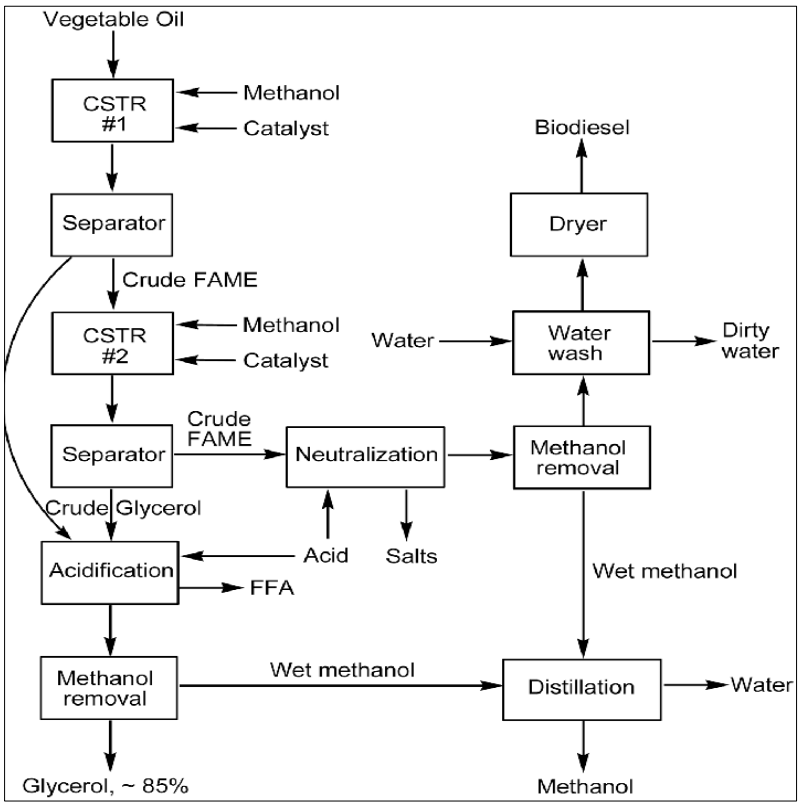

Fig 3: Simplified scheme for industrial biodiesel production from feedstocks with low FFA and water content (Moser, 2010).

Finally, the mapping and selection function links explicitly to key performance indicators that guide continuous improvement. Conversion yield is forecast by correlating quality attributes to reactor performance under site-specific operating envelopes. Carbon intensity spans transport distances, storage losses, and pretreatment energy, not only reaction energy. Energy return on energy invested includes the embodied energy of collection and processing infrastructure alongside solvent recovery efficiencies and heat integration. Unit production cost consolidates procurement, pretreatment, conversion, separation, and compliance costs and is reported both per litre and per megajoule to enable cross-fuel comparison (Hanachi, *et al*., 2015, Kyprianidis, *et al*., 2012). By continuously refining feedstock maps, enforcing rigorous multi-criteria screening, and sustaining cradle-to-gate traceability, the biodiesel regeneration system turns heterogeneity from a liability into a managed variable, stabilizes plant operations, and improves environmental and economic outcomes across rural and urban supply chains.

2.2. Pre-Treatment & Standardization

Pre-treatment and standardization convert heterogeneous, risk-laden inputs into predictable, reactor-ready feeds that meet tight specifications for water, acidity, contaminants, and rheology. The operations sequence begins with coarse and fine filtering to remove particulates that accelerate pump wear, foul heat exchangers, and generate interfacial instability during transesterification. Basket strainers and self-cleaning screen filters with descending mesh sizes (for example 1,000 µm to 100 µm to 10 µm) are arranged in parallel duplex housings to allow maintenance without halting flow. For used cooking oil and animal fats, a heated receiving manifold maintains viscosity below transfer limits and improves capture of settleable solids in conical-bottom tanks. Centrifugal polishing follows for streams with high suspended-load variance; variable-speed decanters paired with disk-stack clarifiers separate fines, entrained water, and heavy impurities with minimal chemical addition (Fahd, *et al*., 2012, O'Connell & Haritos, 2010).

Drying is essential to suppress hydrolysis and saponification. Gravity separation removes free water, but bound moisture requires thermal or vacuum drying. Thin-film evaporators or flash vessels under moderate vacuum achieve low residence time, mitigating thermal cracking and preserving neutral oil quality. Dryer setpoints and hold times are set to achieve moisture control targets (for example ≤0.05–0.10% w/w for transesterification, tighter for base-catalyzed routes), recorded by in-line capacitance probes verified against Karl Fischer titration. For fats that solidify at ambient conditions, jacketed tanks, scraped-surface heat exchangers, and controlled ramping avoid hotspot polymerization while enabling water removal and consistent feed rheology (Caicedo, Barros & Ordás, 2016, Naik, *et al*., 2010).

Degumming targets phospholipids and trace metals that poison catalysts and complicate downstream separations. An acid or water degumming step hydrates gums that are then separated by centrifugation; enzymatic variants reduce chemical usage and sludge volume, but cycle times must be matched to plant takt and storage constraints. When phosphorus is especially problematic (e.g., crude vegetable oils), adsorptive media bleaching earths or modified clays are dosed with careful attention to metal content and ash carryover. Filtration of spent adsorbents via pressure leaf filters restores clarity and protects membranes and catalysts downstream.

Deacidification protects base catalysts and reduces soap formation. Route selection depends on initial free fatty acid (FFA) levels, methanol recovery economics, and co-product strategies. For low to moderate FFA, caustic neutralization

can be applied, creating a soapstock that is acidulated for fatty acid recovery; however, this raises wastewater load and can entrain neutral oil. For high-FFA feeds typical of used cooking oil, acid esterification using sulfuric or solid acid catalysts converts FFA to esters while consuming water; operating at controlled alcohol-to-acid ratios and removing generated water via reactive distillation or pervaporation prevents equilibrium stalls (Menon & Rao, 2012, Mohan, *et al*., 2019). Solid acid resins reduce neutralization requirements and facilitate catalyst separation, but resin fouling necessitates pre-filtration and metals control. Where feasible, counter-current methanol wash reactors improve mass transfer, and closed-loop solvent recovery keeps methanol losses and carbon intensity in check.

Particle-size reduction applies primarily to pre-lipidized residues or embedded solids. For lignocellulosic intermediates or fat-laden sludges, controlled milling or maceration improves heat and mass transfer in subsequent phase separation and extraction operations. Care is taken to avoid generating fines that challenge filtration; rotor–stator devices with adjustable gaps and low-shear screws balance dispersion and downstream filterability.

Inhibitor removal is a continuous theme across the train. Trace metals such as Na, K, Ca, Mg, and transition elements catalyze polymerization, foul membranes, and deactivate catalysts. A mixed strategy of acid wash (for soaps and alkaline metals), ion-exchange polishing (for multivalent cations), and adsorbent beds (for phosphorous and color bodies) achieves parts-per-million targets appropriate for the chosen catalytic route. Soap control begins with upstream oxidation management and low-shear pumping, then relies on controlled neutralization and brine splitting to break emulsions without excessive caustic usage (Naylor & Higgins, 2018, Ong & Bhatia, 2010). Where soaps persist, membrane demulsification or temperature-step centrifugation clears the interface, protecting methanol recovery columns and esterification reactors. Figure 4 shows biomass feedstocks and their utilization in the production of biofuels, bioenergy and bioproducts presented by Welker, *et al*., 2015.

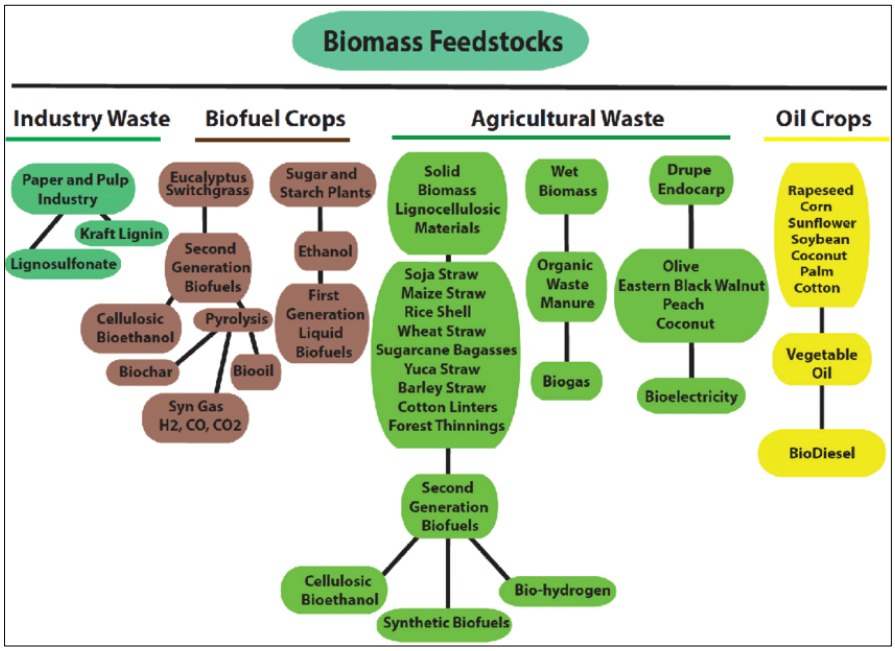

Fig 4: Biomass feedstocks and their utilization in the production of biofuels, bioenergy and bioproducts (Welker, *et al*., 2015).

Moisture control targets are codified as acceptance criteria and alarm limits. Online near-infrared and microwave moisture sensors provide continuous readings, while periodic Karl Fischer measurements serve as reference. Control loops adjust dryer duty, vent rates, and recycle ratios to maintain steady-state moisture below the threshold chosen for base or acid paths. Tank farm procedures enforce water bottom checks, desludging intervals, and nitrogen blanketing to limit atmospheric moisture ingress and oxidation.

In-line characterization underpins the entire pre-treatment philosophy. Soft sensors estimate FFA from correlations between conductivity, density, and temperature-compensated refractive index, but laboratory confirmation via titration or mid-IR spectroscopy calibrates the models and prevents drift. Viscosity is monitored with in-line rotational or vibrating-element viscometers; trends flag polymerization or incomplete melting of fats and indicate when heating profiles need adjustment. Real-time particle counts and differential pressure across filters quantify solids load and predict filter changeovers (Clark, Luque & Matharu, 2012, Lee, *et al*., 2019). For color and oxidation state, UV–Vis absorbance and peroxide value spot checks inform adsorbent dosing and storage handling. Data from these instruments feed a statistical process control (SPC) dashboard with rule-based alerts (for example, Westgard rules), ensuring deviations trigger corrective action rather than propagate variability downstream.

Batching strategy reconciles heterogeneous lots with steady reactor demands. Upon receipt, every lot is sampled with composite protocols that account for stratification and thermal gradients. Lots are tagged with digital identifiers, quality attributes, and uncertainty bounds and then assigned to conditioned buffers. A blending algorithm selects compatible lots to meet target FFA, moisture, and metals before feeding esterification or transesterification trains, minimizing corrective chemicals and maximizing yield. For example, moderate-FFA oil can dilute an extreme-FFA lot to stay within the optimal window for a solid acid reactor,

lowering acid consumption and residence time. Constraint-aware blending also respects viscosity and pour point limits to keep pumps within their operating envelopes and to maintain heat-exchanger approach temperatures (Aref, 2012, Sayyaadi & Mehrabipour, 2012).

Operationally, pre-treatment is governed by standard operating procedures that formalize sampling, instrument calibration, media change criteria, and waste handling. Sludges from degumming and neutralization routes are quantified and routed to valorization or compliant disposal, with mass balance closure checked against tank inventories and meter totals. Solvent usage and recovery are tracked to drive continuous improvement in carbon intensity and cost. Preventive maintenance loops seal inspections, heater descaling, centrifuge bowl cleaning are scheduled from run-hour counters and condition monitoring to sustain uptime. Worker safety is embedded through closed transfer, splash protection, and acid/caustic handling training, complemented by ventilation and off-gas scrubbing around dryers and esterification vessels (Carrasco & Lima, 2017, Hamilton, 2014).

The payoff from rigorous pre-treatment and standardization is measurable. Stable, low-moisture, low-FFA, low-metals feeds translate to narrower reactor operating windows, reduced soap formation, higher phase-separation efficiency, and longer catalyst and membrane lifetimes. Methanol and energy consumption fall as fewer corrective steps are needed, while by-product streams especially glycerol carry less ash and color, expanding upgrading options. Most importantly, in-line characterization and intelligent batching transform feedstock heterogeneity from a chronic liability into a managed variable, enabling predictable yields, lower carbon intensity, improved energy return on energy invested, and more competitive unit costs. In a modular, circular biodiesel regeneration system that draws on diverse agricultural and urban resources, this pre-treatment discipline is what makes flexibility bankable and sustainability claims auditable.

2.3. Conversion Pathways & Catalytic System

Conversion in a modular biodiesel regeneration plant is organized around two coordinated pathways that align chemistry with feedstock acidity. Low-FFA streams refined vegetable oils, conditioned animal fats, and blends stabilized by pre-treatment below about 1–2% FFA enter a base-catalyzed transesterification train that maximizes reaction rate and minimizes alcohol demand. High-FFA streams typical of degraded used cooking oils, soapstock, and certain rendered fractions are first routed to acid esterification to reduce free acids to below the soap-forming threshold, after which they transition to transesterification for triglyceride conversion. This split-routing blueprint protects catalysts, compresses residence times, and stabilizes downstream separations while preserving the flexibility to accommodate daily variation in feed chemistry (Hendricks & Gray, 2019, Stokes, Simpson & Maier, 2014).

In the base train, triglycerides react with methanol or ethanol to form fatty acid alkyl esters and glycerol. With excess alcohol in the dispersed phase, the kinetics are well described as pseudo-first-order in triglyceride; accordingly, vigorous dispersion and interfacial renewal are essential to minimize external mass-transfer resistance. Representative operating envelopes use a 6:1 to 9:1 alcohol-to-oil molar ratio for methanol systems, 0.3–1.0 wt% homogeneous alkali (NaOH or KOH) relative to oil for low-FFA feeds, and 1–5 wt% solid base relative to carrier when employing heterogeneous catalysts such as CaO, MgO, hydrotalcites, or mixed oxides. Temperatures typically sit between 50 and 65 °C for methanol to remain below its atmospheric boiling point while accelerating kinetics; residence times of 10–60 minutes are achievable in well-mixed reactors when moisture and residual FFA are controlled. Phase disengagement after reaction is facilitated by limiting soap formation, controlling shear late in the batch, and maintaining an alcohol ratio high enough to keep viscosity low but not so high that recovery columns are overburdened (Chai & Yeo, 2012, Ibrahim, *et al*., 2017).

The acid train targets high-FFA feeds via esterification using homogeneous acids (sulfuric, p-toluenesulfonic) or heterogeneous solid acids (sulfonated carbons, sulfated zirconia, supported heteropolyacids). Because esterification is equilibrium-limited and slower than base transesterification, operating envelopes deploy higher alcohol ratios often 12:1 to 20:1 methanol-to-acid equivalents temperatures from 60 to 120 °C, and residence times of 30–180 minutes depending on catalyst form and mixing intensity. Light pressurization keeps methanol in liquid phase and permits temperatures above atmospheric boiling, while integrated dehydration via reactive distillation, pervaporation, or membrane vapor permeation removes the water co-product, shifts the equilibrium, and suppresses back-hydrolysis. Once the FFA target (commonly ≤0.5–1.0%) is achieved, the stream is handed off to the base train to complete triglyceride conversion at higher space-time yields (Kyprianidis, 2019, Saboohi, Ommi & Akbari, 2019).

Bifunctional solid acid–base catalysts provide a unified pathway for feeds with mixed requirements, enabling sequential or concurrent esterification and transesterification on a single material. Architectures include acid-functionalized mesoporous silica decorated with basic oxides, layered double hydroxides bearing sulfonic groups, and ZrO_2–Al_2O_3 composites co-doped to present Brønsted and Lewis sites. These materials tolerate moderate moisture and FFA, mitigate soap formation, and simplify workup by eliminating neutralization steps. Their operating windows typically use alcohol-to-oil ratios in the 8:1–12:1 range, temperatures of 60–90 °C, and space velocities adjusted to balance simultaneous reaction pathways; while intrinsic rates may be lower than single-function homogeneous systems, the reduction in wastewater, salt formation, and catalyst handling can improve overall plant economics (Akomea-Agyin & Asante, 2019, Awe, 2017, Osabuohien, 2019).

Process intensification augments both trains. Ultrasound introduces cavitation that produces micro-jets and transient high-shear zones, renewing boundary layers on catalyst surfaces and dispersing alcohol into micron-scale droplets; tuned appropriately, power density and duty cycle can reduce residence time by 30–50% and lower catalyst dosage without damaging equipment. Microwave heating couples directly into polar methanol and intermediate species, flattening temperature gradients, accelerating ramp-up, and enabling precise thermal control; attention to reactor materials prevents hotspots and arcing (Akpan, *et al*., 2017, Oni, *et al*., 2018). Reactive distillation combines reaction and separation, continuously removing methanol-rich vapors or water to drive equilibria toward ester formation, shrinking equipment count and methanol losses. Where solid catalysts are used, spinning-basket or rotating-packed-bed reactors intensify mass transfer at low energy input and allow rapid

catalyst change-out.

Operating envelopes are implemented as recipes linked to real-time analytics that track free acidity, moisture, viscosity, and glycerol. Alcohol-to-oil ratio is the master lever for both rate and separability: higher ratios reduce viscosity and mass-transfer limitations but increase solvent recovery energy; the optimizer therefore enforces a floor to guarantee pseudo-first-order kinetics and a ceiling tied to distillation duty and condenser capacity. Temperature selection approaches kinetic asymptotes without exceeding elastomer, seal, or catalyst stability limits; for methanol systems this often means 55–65 °C in base trains and 70–110 °C in acid or bifunctional trains under modest pressure (Awe & Akpan, 2017). Residence time is set by the slower of chemical conversion and phase disengagement; online conversion estimates (via mid-IR or Raman) and turbidity/particle sensors enable adaptive control. Catalyst regeneration is scheduled proactively based on pressure drop, activity indicators, and soft-sensor estimates of site coverage. Solid bases deactivate via carbonation with CO_2, leaching in alcohol–water mixtures, and poisoning by phosphates and metal soaps; regeneration uses solvent washing to remove adsorbates followed by controlled calcination to restore basicity while avoiding sintering. Solid acids foul with polymerized organics and may slowly lose acidity; regeneration combines solvent washing, mild oxidative treatment, and, for sulfonated carbons, occasional re-sulfonation. Bifunctional materials require balanced protocols that preserve both acid and base functionality (Akpan, Awe & Idowu, 2019, Ogundipe, *et al*., 2019).

Separation choices interact tightly with conversion recipes. After each reaction stage, three-phase centrifuges or settlers split crude FAME, glycerol-rich phase, and rag. Alcohol is flashed from both organic and polar phases and recycled with water control to protect catalyst sites and maintain specified alcohol-to-oil ratios in subsequent stages. Crude glycerol is neutralized, polished, and routed to upgrading, while the ester stream is washed (water or brine), ion-exchanged, or membrane-filtered to remove trace catalyst, soaps, and metals that would otherwise challenge ASTM/EN fuel specifications and poison downstream catalysts (Awe, Akpan & Adekoya, 2017, Osabuohien, 2017). In acid and bifunctional routes, integrated dehydration limits water carryover, protecting base steps and reducing methanol recycle drying load. When membranes are used for alcohol or water management, flux decline is mitigated by pre-filtration and periodic back-pulsing aligned with reactor cycles.

Reactor selection reflects catalyst form, fouling risk, and control strategy. Homogeneous base routes favor agitated CSTRs with static mixers to improve dispersion; staging in series approaches plug-flow behavior and reduces variance in outlet composition. Solid-catalyst routes employ fixed beds with liquid upflow to mitigate channeling and allow on-stream solvent regeneration, oscillatory baffled reactors to decouple mixing from net flow, or rotating packed beds to intensify mass transfer in compact hardware. Safety systems address methanol flammability and toxicity, esterification pressure, and exotherm control; inert-gas blanketing, pressure relief, and gas detection are standard, while interlocks tie heater duty to verified flow to avoid dry-fire incidents (Patrick, *et al*., 2019).

Ultimately, the conversion section translates standardized yet still variable feeds into on-spec biodiesel at high yield, low carbon intensity, and competitive cost by matching esterification/transesterification trains to feed acidity, adopting bifunctional solids where they simplify workup, and applying ultrasound, microwave, and reactive distillation where they shift bottlenecks. Operating envelopes alcohol-to-oil ratio, temperature, residence time, and catalyst regeneration cadence are not static setpoints but adaptive policies driven by analytics and economics. This dynamic control keeps the plant inside quality constraints while minimizing methanol loss, energy consumption, and downtime, delivering a resilient and bankable pathway for biodiesel regeneration across diverse agricultural and urban supply chains.

2.4. Separation, Purification & By-product Valorization

Separation, purification, and by-product valorization transform chemically converted intermediates into fuel that consistently meets ASTM D6751 and EN 14214 while turning side streams into revenue and minimizing waste liabilities. The first task after reaction is a reliable phase split. For most recipes, crude fatty acid methyl/ethyl esters coexist with a polar phase rich in methanol, glycerol, soaps, and dissolved salts, with a rag layer of emulsified fines. A membrane-based split or high-g field centrifugation can execute this partition with minimal residence time. Three-phase disc-stack centrifuges, fitted with adjustable paring discs, continuously discharge light ester, heavy glycerol, and rag; bowl speed and feed temperature are tuned to viscosity and interfacial tension so that droplet coalescence is not rate limiting (Bankole, *et al*., 2019, Nwokediegwu, Bankole & Okiye, 2019). Where energy and maintenance budgets favour lower shear, membrane separators use hydrophilic channels to wick the glycerol-rich phase while rejecting the ester phase; upstream 10–1 μm polishing prevents pore blinding, and periodic back-pulse cycles synchronize with reactor batches. Either route benefits from modest heat (45–55 °C) to reduce viscosity, controlled shear to avoid fresh emulsions, and in-line demulsifier or electrolyte dosing when soap burdens are high.

Methanol and solvent recovery loops are the financial and environmental hinge of the plant. Alcohol is present in both phases after the split; stripping and rectification capture it to near-azeotropic purity for recycle. A two-stage flash on the ester stream removes bulk methanol at mild vacuum; the overheads flow to a rectifier where heads (water-rich) are purged or reprocessed and hearts (dry methanol) return to the feed surge. On the glycerol side, a flash followed by decantation separates residual esters, and reactive wash or salt-split collapses soaps before rectification. To cut reboiler duty and condenser loads, heat integration pairs the hot bottoms of rectifiers with preheating of reactor feeds, while mechanical vapour recompression is considered at larger scales (Atobatele, *et al*., 2019, Filani, Nwokocha & Babatunde, 2019). Where water co-product or ingress burdens the column, organophilic pervaporation modules selectively permeate methanol over water, trimming the dehydration load and protecting catalysts from water in subsequent passes.

Once methanol is under control, the ester stream advances to polishing to lock in conformity with fuel specifications on water, total contamination, residual glycerides/glycerol, acidity, oxidation stability, and metals. Traditional wet wash with water or brine remains effective for removing soaps and residual catalyst, but it generates effluent that must be treated. Dry-wash trains avoid effluent by using adsorbents and ion

exchangers. Magnesium silicate, modified clays, and polymeric resins scavenge soaps, trace water, and colour bodies; mixed-bed cation/anion exchangers reduce Na, K, Ca, and Mg below the ppm thresholds that otherwise compromise injector life and aftertreatment systems (Aduwo & Nwachukwu, 2019, Erigha, *et al*., 2019). Deep eutectic solvents (DES) add a tunable, green layer to polishing. Hydrogen-bonded liquids such as choline chloride:glycerol, choline chloride:urea, or betaine-based systems can be engineered to selectively complex soaps, free fatty acids, and metal ions while showing low volatility and high thermal stability. In a contactor stage, a measured DES ratio extracts inhibitor; phase disengagement is rapid due to immiscibility with FAME at process temperature, and the spent DES is regenerated by mild water washes or electro-membrane steps that recover the captured species. Because DES formation can employ glycerol from the process as the hydrogen-bond donor, the plant closes a loop, reducing purchased solvent demand and improving carbon intensity. Final filtration (0.45–1.0 μm), followed by vacuum drying or membrane dewatering to bring water ≤500 mg/kg (or per local spec), ensures storage stability and corrosion control. Inline mid-IR, conductivity, and density checks verify monoglyceride and total glycerol limits, while ICP-OES sampling of metals after the ion-exchange skid confirms compliance (Atobatele, Hungbo & Adeyemi, 2019).

Managing the rag layer and soap-rich streams is a frequent bottleneck. A controlled acidulation splits soaps into free fatty acids that can be recycled to the esterification step, minimizing neutral oil loss and effluent. Where emulsions persist, temperature-stepped centrifugation and membrane demulsification reduce residence time and chemical use. Spent adsorbents are drained and steam-stripped to recover occluded esters; life extension through low-temperature regeneration ovens and occasional solvent washing cuts disposal tonnage. Filter cakes and fines are quantified into the site-wide mass balance so that carbon accounting and waste permits remain accurate and auditable.

Crude glycerol, the principal by-product, dictates the economics of valorization and the credibility of zero-waste claims. Its composition depends on catalysis and washing: 50–85 wt% glycerol with methanol, water, salts (from neutralization), soaps, and colour bodies. The first step is neutralization and salt management: acidification collapses soaps to fatty acids (recycled), while controlled base/acid swings and settling minimize ash. A methanol strip brings alcohol back to the rectifier, and carbon/ion-exchange polishing prepares streams for higher-value pathways. One route targets epoxides and epichlorohydrin production via glycerol hydrochlorination and dehydrochlorination; modern catalysts and HCl recycle reduce chlorine usage and produce an epoxide feedstock for epoxy resins (Bankole & Tewogbade, 2019, Fasasi, *et al*., 2019). A second route converts glycerol with urea or dimethyl carbonate to glycerol carbonate under tin or heterogeneous base catalysis; the product is a valuable reactive solvent and monomer intermediate that can be further transesterified to bio-based polycarbonates. Solketal formation by acetone acetalization over solid acids yields an oxygenate and octane booster, with downstream distillation cutting to fuel-grade blends.

Biological valorization unlocks polymer and chemical platforms while tolerating residual impurities. Select microbial consortia convert glycerol to 1,3-propanediol, succinic acid, or polyhydroxyalkanoate (PHA) biopolymers in fed-batch reactors; salts and residual methanol are managed by upstream polishing and optimized nutrient ratios. Sludge from fermentation is dewatered and can be composted or anaerobically digested. Thermocatalytic routes aqueous-phase reforming or steam reforming generate hydrogen-rich gas; after water-gas shift and PSA cleanup, H_2 feeds hydrotreaters, fuel cells, or ammonia loops. Waste heat from reformers integrates with methanol recovery and dryer duties, while captured CO_2 from the PSA tail can be fed to algae or mineralized into carbonates (Atobatele, Hungbo & Adeyemi, 2019, Hungbo & Adeyemi, 2019). Where markets support it, technical-grade glycerol purification via vacuum distillation and thin-film evaporators reaches USP-adjacent specifications, enabling sales into personal-care or resin markets with appropriate QA.

Waste minimization wraps around each unit. Brine from wet wash is recycled as make-up where ionic strength is required for emulsion breaking; counter-current configurations reduce freshwater intensity. Ion-exchange resins are regenerated with optimized acid/base cycles captured in a closed loop; eluates are blended to the acidulation system to recover fatty acids and reduce neutral-salt discharge. Spent DES is rejuvenated and monitored with conductivity and viscosity before return to service; only end-of-life fractions with accumulated heavy metals are sent for hazardous waste treatment. Distillation bottoms are balanced against fouling risk and reintroduced to the acidification train when feasible, recovering organics that would otherwise inflate disposal cost. Nitrogen blanketing on storage, antioxidant dosing aligned with peroxide value tracking, and low-oxygen pumps preserve ester stability and extend inventory life, cutting spoilage (Atobatele, Hungbo & Adeyemi, 2019, Hungbo & Adeyemi, 2019).

The purification train ends where storage and loading begin, but quality assurance is ever-present. Each lot closes with a certificate of analysis covering acid number, ester content, residual alcohol, total and free glycerol, monoglyceride/diglyceride levels, water, density, cold filter plugging point or cloud point, sulfur, metals, and oxidation stability (e.g., Rancimat). Deviation triggers are built into the execution system: if metals approach limits, ion-exchange bed switching advances; if water trends upward, membrane dewatering duty increases; if monoglycerides spike, residence time or temperature in the finishing reactor is adjusted. This coupling of separation/polishing with analytics ensures that fuel leaves the gate compliant and that rework is the exception, not the norm (Filani, Nwokocha & Babatunde, 2019, Kamau, 2018).

By embedding efficient phase separation, low-loss solvent recovery, smart polishing including deep eutectic solvent extraction and disciplined by-product valorization, the conceptual model converts a messy reaction effluent into two coherent value streams: on-spec biodiesel and upgraded co-products. The former achieves reproducible quality with a declining carbon and water footprint; the latter whether as epoxides, glycerol carbonate, solketal, PHA precursors, or hydrogen improves plant margins and resilience. Waste is squeezed into smaller, more benign fractions through regeneration, recycle, and integration, and the site-wide mass and energy balances remain tight enough to withstand audits and credit program scrutiny. In a diversified feedstock reality, this closing section is what transforms flexible chemistry into bankable operations.

2.5. Cyber-Physical Control & Optimization

The cyber-physical control and optimization layer closes the loop between physical biodiesel production processes and intelligent decision systems, ensuring efficient, safe, and high-quality operation at all times. In this model, sensors, controllers, and analytics modules converge into an integrated network that continuously perceives, predicts, and optimizes plant behavior. The central objective is to achieve energy-efficient conversion, consistent product quality that meets ASTM/EN standards, and operational uptime exceeding 95%, even under variable feedstock conditions and environmental disturbances.

At the core of this layer are soft sensors and hybrid models that combine first-principles thermodynamic and kinetic equations with data-driven machine-learning (ML) components. First-principles models describe reaction kinetics, heat and mass transfer, phase equilibria, and solvent recovery under known physical constraints. They capture the stoichiometry of esterification/transesterification, vapor–liquid equilibria in methanol–oil–water systems, and the energy balances across heat exchangers and dryers. However, the complexity of real feedstock mixtures containing variable moisture, free fatty acids, and contaminants introduces nonlinearities and unmodeled dynamics (Ayanbode, *et al*., 2019, Onalaja, *et al*., 2019). ML models bridge this gap by learning empirical corrections from plant data. Neural networks, random forests, and Gaussian-process regressors are trained on historical batches and simulated datasets to estimate hidden variables such as FFA, viscosity, or catalyst deactivation rate based on measurable signals like temperature, conductivity, density, torque, and differential pressure. These soft sensors reduce dependency on manual laboratory assays, offering real-time estimates of key quality indicators.

The hybrid structure integrates mechanistic and statistical elements through co-simulation or digital twin frameworks. For example, the reactor model predicts baseline conversion, while an ML residual corrector adjusts the prediction according to sensor drift or unmeasured impurities. Bayesian updating continuously refines model parameters as new data arrive, ensuring the hybrid model remains valid across feedstock seasons. In parallel, sensor fusion algorithms combine infrared spectroscopy, capacitance moisture meters, and flow-viscosity sensors to estimate compositional states. Outlier detection and auto-calibration routines guard against sensor fouling, drift, or misalignment, maintaining trust in digital measurements that drive control decisions (Seyi-Lande, Oziri & Arowogbadamu, 2019).

Advanced model-predictive control (MPC) sits atop this data foundation. MPC uses an explicit dynamic model of the plant to forecast future behavior over a moving horizon and optimize control inputs while respecting constraints. In the biodiesel regeneration context, it simultaneously manipulates heating rates, catalyst dosing, alcohol-to-oil ratios, recycle flows, and separation pressures to minimize total energy consumption and deviation from quality specifications. The controller solves a quadratic or nonlinear optimization problem every few seconds, balancing economic objectives yield, carbon intensity, and solvent recovery against safety and operational limits. Real-time optimization layers integrate cost functions such as energy price, methanol recovery rate, and EROEI contribution (Akinrinoye, *et al*. 2019, Didi, Abass & Balogun, 2019, Otokiti & Akorede, 2018).

The MPC framework also manages process uptime by embedding reliability constraints. Predictive maintenance data feed into the optimization model: bearing temperature, vibration spectra, and filter differential pressures are treated as soft constraints with penalties that grow as components near degradation thresholds. When these indicators exceed risk levels, the controller shifts operating conditions to reduce stress lowering centrifuge speed, modulating heat-exchanger duty, or lengthening reaction residence times thus sustaining uptime beyond 95% without abrupt shutdowns. Fault-detection and isolation modules employ parity equations and ML classifiers to distinguish between sensor errors, actuator faults, and true process anomalies, triggering graded responses from alarm to automatic bypass (Akinbola & Otokiti, 2012, Dako, *et al*., 2019, Oziri, Seyi-Lande & Arowogbadamu, 2019).

Energy management is tightly coupled with control optimization. Real-time energy balances are computed from steam, electricity, and cooling utilities, with MPC scheduling loads to align with renewable power availability or tariff periods. Heat integration networks are digitally supervised to maintain approach temperatures and prevent exchanger fouling. When a heat-recovery unit exhibits declining performance, soft sensors in the twin predict fouling thickness and the associated penalty on energy efficiency; MPC then compensates by adjusting upstream flow splits or scheduling clean-in-place cycles during off-peak hours.

A plant-wide supervisory digital twin unifies all these elements into a living, continuously learning representation of the biodiesel regeneration system. The twin mirrors every reactor, separator, and energy exchanger through synchronized data streams and dynamic simulation models. It executes sensitivity analyses to determine which variables most influence conversion efficiency, carbon intensity, and product purity, guiding instrumentation investments and control tuning. Uncertainty analysis uses Monte Carlo or polynomial-chaos methods to propagate measurement and model uncertainties through the process, generating confidence intervals for KPIs such as yield and carbon intensity (Ajonbadi, *et al*., 2014, Didi, Balogun & Abass, 2019, Farounbi, *et al*., 2019). Operators visualize these intervals in dashboards, enabling risk-aware decision-making rather than point-value reliance.

Fouling prediction is a special function within the digital twin. By analyzing temperature differentials, flow velocity, and historical cleaning records, ML models forecast fouling rates in heat exchangers, membranes, and centrifuges. For membranes, transmembrane pressure rise and flux decline curves feed a recurrent neural network that estimates remaining useful life and optimal backwash intervals. For heat exchangers, regression models trained on pressure-drop and outlet-temperature data predict fouling resistance, allowing proactive cleaning before efficiency loss escalates. These forecasts feed into MPC's planning horizon so that maintenance and energy optimization occur cohesively rather than reactively.

The cyber-physical architecture rests on industrial Internet of Things (IIoT) infrastructure with redundant data pathways. Edge devices collect sensor data at sub-second resolution and perform local preprocessing filtering, compression, and health checks before transmission to the central historian. The historian maintains time-series databases accessible to analytics engines and visualization tools. Cybersecurity layers include encrypted communication, role-based access,

and anomaly detection to prevent malicious control manipulation. In critical loops, local controllers maintain safe fallback logic in case of network disruption (Balogun, Abass & Didi, 2019, Otokiti, 2018, Oguntegbe, Farounbi & Okafor, 2019).

Machine-learning components within the control hierarchy are governed by explainability and validation routines. Before a new model is deployed, it undergoes cross-validation against unseen datasets and a "shadow mode" run where its predictions are compared with legacy control decisions without influencing the plant. Only when consistency and benefit are proven does the supervisory system authorize model activation. Drift detection monitors performance metrics such as prediction error or yield deviation; if these metrics exceed limits, automatic retraining or reversion to the previous model occurs.

Operator interaction with the cyber-physical system is designed for transparency and trust. Dashboards display real-time process maps with overlaid KPIs energy intensity, conversion yield, carbon intensity, methanol recovery, and uptime along with predictive alerts for fouling or catalyst deactivation. Explainable AI modules translate control actions into human-readable rationales, linking them to energy savings or risk mitigation. Decision support tools allow operators to test "what-if" scenarios such as altered feedstock mix or methanol price change by running the digital twin in predictive mode. The outcomes guide production planning and market hedging strategies (Ajonbadi, Mojeed-Sanni & Otokiti, 2015, Evans-Uzosike & Okatta, 2019, Oguntegbe, Farounbi & Okafor, 2019).

Integration with enterprise systems extends optimization beyond the plant floor. The digital twin exchanges data with supply-chain and sustainability platforms to compute real-time carbon accounting and generate verifiable emission reports. Feedstock variability predictions from the procurement module adjust reactor schedules and catalyst regeneration plans; conversely, energy consumption data feed into sustainability dashboards that track ISO 14064 and ESG compliance metrics. By bridging operational and corporate layers, the cyber-physical system ensures that process optimization translates directly into economic and environmental performance gains.

The impact of such integrated control is profound. Real-time soft-sensor feedback shortens response times to disturbances such as moisture spikes or catalyst activity loss, preventing off-spec production. Hybrid models capture both the physics of reaction and the uncertainty of raw material behaviour, maintaining product quality within tight ASTM/EN bounds. MPC aligns energy, quality, and reliability goals rather than trading them off, delivering a consistently low carbon intensity and high EROEI. The digital twin transforms the plant into a continuously learning organism that understands its own sensitivities, quantifies uncertainty, and anticipates fouling or failure before they impair operations (AdeniyiAjonbadi, *et al*., 2015, Didi, Abass & Balogun, 2019, Umoren, *et al*., 2019).

Ultimately, cyber-physical control and optimization redefine biodiesel regeneration from static batch chemistry to adaptive industrial intelligence. The combination of physics-based insight, machine-learning foresight, and predictive control ensures that each litre of biodiesel is produced with minimal waste, optimal energy use, and verified sustainability. Uptime beyond 95%, reduced methanol loss, stabilized catalyst life, and transparent digital traceability become not aspirational metrics but standard operating outcomes hallmarks of a resilient, data-driven circular energy system capable of thriving in an increasingly variable bioeconomy.

2.6. Sustainability, Safety & Techno-Economic Assessment

Sustainability, safety, and techno-economic assessment form the evidentiary backbone of a biodiesel regeneration model, converting engineering intent into quantified performance, verified risk controls, and financeable outcomes. A dynamic life-cycle assessment captures how carbon, water, and eutrophication footprints evolve with feedstock mix, operating mode, and learning-curve improvements, while a techno-economic analysis converts design choices into CAPEX, OPEX, payback, and risk-adjusted returns. Health, safety, and environmental management stitches these threads together by identifying hazards, implementing safeguards, and ensuring waste and emissions compliance under realistic operating disturbances. Finally, market and policy levers renewable credits, carbon pricing, and sustainable procurement translate environmental performance into revenue and demand, closing the loop between sustainability metrics and cash flow (Ajayi, *et al*., 2019, Bayeroju, *et al*., 2019, Sanusi, *et al*., 2019).

The dynamic LCA is structured around modular unit processes collection, pretreatment, conversion, solvent recovery, separation, polishing, and by-product upgrading parameterized by time-varying inputs. Carbon intensity per megajoule of fuel is computed cradle-to-gate, with transport emissions tied to route length and payload utilization; pretreatment energy depends on measured moisture removal duty; conversion contributes via heat and electricity intensity and methanol makeup; and credits are applied for co-products such as refined glycerol, solketal, glycerol carbonate, or hydrogen when system expansion or substitution is defensible. Water intensity separates blue water (process and cooling) from gray water (effluent assimilation capacity), and eutrophication potential aggregates nutrient discharges from wet-wash streams, brine regeneration, and accidental losses. Because feedstock composition and operations fluctuate, the LCA runs in rolling windows, updating inventories from plant historians and soft sensors. Uncertainty bands are generated via Monte Carlo sampling of key parameters diesel displacement factor, electricity grid intensity, solvent recovery rates, and logistics distances and reported alongside point estimates so that decisions are risk-aware rather than nominal (Ajayi, *et al*., 2018, Bukhari, *et al*., 2018, Essien, *et al*., 2019).

TEA translates the same process map into cost and value. Capital costs include tankage with heating and insulation, filters and centrifuges, thin-film or vacuum dryers, esterification and transesterification reactors (including solid-catalyst hardware), rectification and pervaporation modules for solvent loops, polishing skids (adsorbents, ion exchange, membranes), glycerol upgrading trains, utilities, and control systems. Working capital accounts for methanol inventory, catalyst and adsorbent cycles, and spare parts. Operating costs track feedstock purchases net of quality adjustments; energy for heating, cooling, and drives; chemicals (acid/base, adsorbents, resins, antioxidants, demulsifiers); waste handling; labour; maintenance; and compliance monitoring (Akinrinoye, *et al*. 2015, Bukhari, *et al*., 2019, Erigha, *et al*., 2019). The model outputs levelized cost per litre and per megajoule, cash flow over plant life, payback period, net present value, and internal rate of return

under reference and stress scenarios. Sensitivity analysis isolates drivers feedstock price, methanol recovery efficiency, electricity tariff, glycerol netbacks, and capacity factor while scenario analysis overlays policy pathways (credit prices, carbon costs) and logistics shocks. For distributed micro-refineries, economies of scope (shared collection and tele-maintenance) may offset scale limits, whereas mid-scale hubs emphasize heat integration and advanced solvent recovery to compress OPEX. The TEA is explicitly linked to LCA by valuing carbon intensity reductions through credit markets or carbon prices, ensuring that environmental gains register in the pro forma.

Safety and environmental protection are addressed through an HSE framework that begins with systematic hazard identification. Methanol flammability and toxicity, acid/caustic handling during esterification and neutralization, high-temperature operations, pressure in reactive distillation, and confined-space tank entry are primary chemical and process hazards. Mechanical hazards include rotating equipment (centrifuges, pumps), hot surfaces, and pressure relief discharge. Environmental hazards concentrate around VOCs from solvent loops, wastewater from wet washes and resin regeneration, solids from spent adsorbents and filter cakes, and off-gases carrying acid mists or HF traces in edge cases. Safeguards are layered: inherently safer design (closed transfer, nitrogen blanketing, low-inventory methanol manifolds), engineering controls (double-seal pumps with leak detection, LEL gas detection, interlocked heater duty to verified flow, containment curbs, scrubbers on vents, and heat-exchanger approach monitoring to avoid thermal stress), administrative controls (permit-to-work, lockout/tagout, hot-work management, tank entry protocols, and competency training), and emergency response (foam systems, deluge on storage, spill kits, eyewash and showers, and mutual-aid arrangements with local responders). For process safety, relief systems are sized for runaway transesterification exotherms or utility failures, and hazard reviews (HAZOP/LOPA) allocate safety instrumented functions to prevent loss-of-containment (Ajayi, *et al*., 2018, Bukhari, *et al*., 2018, Essien, *et al*., 2019). Waste and emissions compliance is operationalized through online flow and pH monitoring of effluents, COD/BOD sampling, mass-balance reconciliation on salts and metals from neutralization and polishing, and emissions inventories for boilers, flares, and solvent columns; continuous improvement projects target source reduction before end-of-pipe treatment.

The sustainability case is inseparable from by-product management. Glycerol streams are treated as product opportunities rather than disposal problems, with distinct valorization routes matched to quality: epichlorohydrin for epoxy chains, glycerol carbonate as a reactive solvent, solketal as a fuel oxygenate, biological conversion to PHAs or succinic acid, and reforming to hydrogen. Each route has its own hazard and compliance profile chlorinated chemistry requires controlled HCl handling and brine management; catalytic carbonylation demands CO safeguards; fermentation generates nutrient-bearing effluents and these are embedded in the HSE plan. Waste minimization programs quantify and shrink rag, sludge, and spent media via regeneration, and closing loops in solvent systems and deep eutectic solvent polishing reduces volatile emissions and freshwater demand (Kyprianidis, 2019, Saboohi, Ommi & Akbari, 2019). The dynamic LCA credits these improvements in near-real time, incentivizing housekeeping that shows up on the sustainability scorecard.

Policy and market instruments provide the bridge from verified performance to project bankability. In jurisdictions with renewable fuel standards, each litre of biodiesel can generate identification numbers or credits when carbon intensity and feedstock provenance meet pathway requirements; low-carbon fuel standard regimes reward lower-CI fuels with tradable credits valued at market prices. Accurate, auditable CI calculations rely on the same dynamic LCA pipeline, with pathway submissions supported by metered energy, solvent recovery yields, and verified logistics distances. Carbon pricing explicit taxes or cap-and-trade makes energy efficiency and solvent recovery improvements directly accretive to margin; the TEA models a carbon cost on residual emissions and a credit for displacement of fossil diesel, allowing capital ranking by abatement cost per tonne (Chai & Yeo, 2012, Ibrahim, *et al*., 2017). Sustainable procurement guided by ISO 20400 principles creates preferential demand from public and corporate buyers that integrate environmental and social criteria into contracts. The plant's chain-of-custody system, supplier scorecards, and recycled-content and CI claims feed buyer dashboards, enabling verifiable scope 3 reductions. Long-term offtake contracts indexed to credit prices or carbon benchmarks stabilize revenue, while green loans or sustainability-linked debt tie interest margins to KPI performance (energy intensity, CI, wastewater reduction), aligning finance with operational excellence.

Integrating these layers transforms compliance into competitive advantage. Operators use digital twins to anticipate how a hotter, drier season will raise drying duty and CI unless route plans shorten average collection distance; MPC can then shift heat-integration targets and solvent-loop setpoints to preserve carbon performance. HSE analytics mine near-miss reports and condition data to predict when centrifuge vibration trends presage seal failure, scheduling maintenance during low-credit weeks to protect uptime and revenue. TEA dashboards show the breakeven credit price that justifies a pervaporation retrofit, while policy trackers simulate margin impacts from revised credit formulas or grid decarbonization. Social metrics local hiring, small supplier inclusion, and community benefits from waste-oil collection round out the sustainability profile and can be embedded in procurement scoring and ESG reporting (Hendricks & Gray, 2019, Stokes, Simpson & Maier, 2014).

Ultimately, the conceptual model's credibility rests on quantified cause-and-effect. Dynamic LCA ensures that operational decisions and continuous improvement register as verifiable reductions in carbon, water, and nutrient burdens. TEA proves that these reductions are achieved at acceptable cost with resilient returns under realistic volatility. HSE governance keeps people and the environment safe while converting hazards into managed risks. Policy and procurement instruments reward the verified outcomes, lowering the cost of capital and attracting durable demand. Together, these components make biodiesel regeneration from agricultural and urban wastes not only technically feasible but also environmentally material, socially constructive, and financially prudent an integrated pathway from heterogeneous feedstocks to dependable, low-carbon fuel markets (Carrasco & Lima, 2017, Hamilton, 2014).

2.7. Deployment, Governance & Conclusion

Deployment prioritizes a hub-and-spoke network of micro-refineries sited near cluster farms, food-service corridors, rendering plants, and municipal transfer stations, shortening haul distances and stabilizing feed quality while creating local jobs. Each spoke aggregates used cooking oil, animal fats, and crop residues into conditioned lots through filtration, water draw-off, and basic analytics, then backhauls to a nearby hub for esterification, separation, and polishing. Route design uses time-windowed pickup schedules, heat-mapped generation profiles, and dynamic vehicle routing to maximize payload and minimize rehandling; jacketed or insulated tankers service high-tallow routes, IBCs with tamper-evident seals protect small generators, and telemetry validates geofenced pickups to deter adulteration. Hubs are modular skid-mounted pretreatment, esterification/esterification stages, methanol recovery, and polishing so capacity can be right-sized to local supply and incrementally expanded. Standardized utility blocks (steam, chilled water, compressed air), drop-in catalyst packs, and quick-connect manifolds compress commissioning time and allow rapid change-outs. Inter-hub balancing and temporary mobile units absorb seasonal peaks, while shared laboratories and spare-parts pools reduce fixed overhead.

Governance anchors the network in transparency, accountability, and community benefit. A digital chain-of-custody system assigns every batch a unique identifier at first transfer, linking source coordinates, quality attributes, and mass balance through to product shipment and credit claims. Procurement follows ISO 20400 principles, weighting local participation, safety records, and environmental performance alongside price. Community co-ownership structures cooperatives of smallholder suppliers, municipal enterprises, or community benefit trusts take equity or revenue-share positions at the spoke or hub level, aligning incentives for consistent quality and reliable supply. Workforce programs prioritize local hiring, credentialing in process operations and HSE, and career pathways into analytics and maintenance. HSE governance layers inherently safer design (closed transfer, nitrogen blanketing), engineered safeguards (gas detection, interlocks, secondary containment), and disciplined operations (permit-to-work, lockout/tagout, emergency drills), with third-party audits and publicly reported indicators. Data governance specifies role-based access, privacy for supplier commercial data, and auditable MRV pipelines for carbon-intensity and recycled-content claims.

Financing blends concessional and commercial capital to match risk with return across the rollout curve. Early deployments leverage grants, green bonds, or catalytic equity for first-of-kind modules; scale-out phases draw on sustainability-linked loans whose coupons step down as KPIs improve (carbon intensity, water use, solvent recovery, incident rate). Forward sales of RINs/LCFS and offtake agreements with fleets and public buyers de-risk revenue, while insurance wraps cover business interruption and environmental liability. A centralized treasury hedges methanol and energy prices and pools credit exposure across hubs, unlocking lower financing costs than isolated projects could access.

Resilience planning treats feedstock shocks as design conditions rather than exceptions. Supply portfolios are diversified across waste oils, rendered fats, and contracted oilseed fractions, with contractual “switch rules” that reallocate streams as quality or availability changes. Spokes maintain minimum days of cover in conditioned tanks; hubs carry safety stocks of adsorbents, catalysts, and ion-exchange resins sized to historical worst-case variability. Dual-train conversion (acid and base) and bifunctional solid catalysts provide routing flexibility; mobile pretreatment skids can be deployed to emergent hotspots after festivals, harvests, or market shifts. Stress-testing in the digital twin simulates droughts, disease outbreaks, policy pivots, or restaurant density swings, and produces playbooks that adjust routing, blending, and setpoints without breaching quality or cost limits. Mutual-aid pacts enable inter-hub support for spare parts, specialist technicians, and temporary storage during disruptions.

The program closes with disciplined measurement and learning. A concise KPI suite conversion yield, carbon intensity per megajoule, energy return on energy invested, unit cost, methanol recovery rate, water intensity, uptime and overall equipment effectiveness, incident and near-miss rates, recycled-content share, local spend, and jobs supported feeds monthly reviews and annual public reports. Statistical process control and root-cause analysis drive corrective actions; counterfactual experiments in the digital twin verify that observed improvements are attributable to specific interventions. Procurement and financing terms index to KPI outcomes, reinforcing the loop between performance and capital cost.

In conclusion, the conceptual model delivers an integrated blueprint that converts heterogeneous agricultural and urban wastes into dependable, low-carbon biodiesel through modular hub-and-spoke deployment, transparent governance, and community co-ownership. It operationalizes flexibility via standardized hardware blocks, digital chain-of-custody, and adaptive control, and it embeds resilience through diversified supply, inventories sized by stress tests, and dual-path chemistry. Because outcomes are anchored in measurable KPIs yield, carbon intensity, EROEI, cost, solvent and water efficiency, uptime, safety, and social value the system can earn policy credits, attract sustainability-linked finance, and meet the procurement needs of fleets and municipalities. Most importantly, it offers a pathway to scale that is equitable as well as efficient, directing economic value to the communities that generate the feedstock, while delivering verifiable environmental gains and bankable operations. This is biodiesel regeneration not as a niche diversion, but as an auditable, resilient, and inclusive energy service woven into regional agricultural and urban ecosystems.

3. References

1. Abass OS, Balogun O, Didi PU. A predictive analytics framework for optimizing preventive healthcare sales and engagement outcomes. IRE J. 2019;2(11):497-503.
2. Adeniyi Ajonbadi H, Aboaba Mojeed-Sanni B, Otokiti BO. Sustaining competitive advantage in medium-sized enterprises (MEs) through employee social interaction and helping behaviours. J Small Bus Entrep Dev. 2015;3(2):89-112.
3. Aduwo MO, Nwachukwu PS. Dynamic capital structure optimization in volatile markets: a simulation-based approach to balancing debt and equity under uncertainty. IRE J. 2019;3(2):783-92.
4. Ahmadi P, Dincer I. Thermodynamic and exergoenvironmental analyses, and multi-objective

optimization of a gas turbine power plant. Appl Therm Eng. 2011;31(14-15):2529-40. doi:10.1016/j.applthermaleng.2011.04.019.
5. Ajayi JO, Bukhari TT, Oladimeji O, Etim ED. A conceptual framework for designing resilient multi-cloud networks ensuring security, scalability, and reliability across infrastructures. IRE J. 2018;1(8):164-73.
6. Ajayi JO, Bukhari TT, Oladimeji O, Etim ED. Toward zero-trust networking: a holistic paradigm shift for enterprise security in digital transformation landscapes. IRE J. 2019;3(2):822-31.
7. Ajayi JO, Bukhari TT, Oladimeji O, Etim ED. A predictive HR analytics model integrating computing and data science to optimize workforce productivity globally. IRE J. 2019;3(4):444-53.
8. Ajonbadi HA, Lawal AA, Badmus DA, Otokiti BO. Financial control and organisational performance of the Nigerian small and medium enterprises (SMEs): a catalyst for economic growth. Am J Bus Econ Manag. 2014;2(2):135-43.
9. Ajonbadi HA, Otokiti BO, Adebayo P. The efficacy of planning on organisational performance in the Nigeria SMEs. Eur J Bus Manag. 2016;8(24):25-47.
10. Akinbola OA, Otokiti BO. Effects of lease options as a source of finance on profitability performance of small and medium enterprises (SMEs) in Lagos State, Nigeria. Int J Econ Dev Res Invest. 2012;3(3):70-6.
11. Akinrinoye OV, Umoren O, Didi PU, Balogun O, Abass OS. Predictive and segmentation-based marketing analytics framework for optimizing customer acquisition, engagement, and retention strategies. Eng Technol J. 2015;10(9):6758-76.
12. Akomea-Agyin K, Asante M. Analysis of security vulnerabilities in wired equivalent privacy (WEP). Int Res J Eng Technol. 2019;6(1):529-36.
13. Akpan UU, Adekoya KO, Awe ET, Garba N, Oguncoker GD, Ojo SG. Mini-STRs screening of 12 relatives of Hausa origin in northern Nigeria. Niger J Basic Appl Sci. 2017;25(1):48-57.
14. Akpan UU, Awe TE, Idowu D. Types and frequency of fingerprint minutiae in individuals of Igbo and Yoruba ethnic groups of Nigeria. Ruhuna J Sci. 2019;10(1):34-46.
15. Aljamel SAM. A conceptual framework for power generation technology management for developing countries [dissertation]. Sheffield: Sheffield Hallam University; 2010.
16. Al-Yafei EF. Sustainable design for offshore oil and gas platforms: a conceptual framework for topside facilities projects [doctoral dissertation]. Edinburgh: Heriot-Watt University; 2018.
17. Atobatele OK, Ajayi OO, Hungbo AQ, Adeyemi C. Leveraging public health informatics to strengthen monitoring and evaluation of global health intervention. IRE J. 2019;2(7):174-93.
18. Atobatele OK, Hungbo AQ, Adeyemi C. Digital health technologies and real-time surveillance systems: transforming public health emergency preparedness through data-driven decision making. IRE J. 2019;3(9):417-21.
19. Atobatele OK, Hungbo AQ, Adeyemi C. Leveraging big data analytics for population health management: a comparative analysis of predictive modeling approaches in chronic disease prevention and healthcare resource optimization. IRE J. 2019;3(4):370-5.
20. Awe ET. Hybridization of snout mouth deformed and normal mouth African catfish Clarias gariepinus. Anim Res Int. 2017;14(3):2804-8.
21. Awe ET, Akpan UU, Adekoya KO. Evaluation of two MiniSTR loci mutation events in five father-mother-child trios of Yoruba origin. Niger J Biotechnol. 2017;33:120-4.
22. Ayanbode N, Cadet E, Etim ED, Essien IA, Ajayi JO. Deep learning approaches for malware detection in large-scale networks. IRE J. 2019;3(1):483-502.
23. Bankole FA, Tewogbade L. Strategic cost forecasting framework for SaaS companies to improve budget accuracy and operational efficiency. Iconic Res Eng J. 2019;2(10):421-41.
24. Bankole FA, Dako OF, Onalaja TA, Nwachukwu PS, Lateefat T. Blockchain-enabled systems fostering transparent corporate governance, reducing corruption, and improving global financial accountability. Iconic Res Eng J. 2019;3(3):259-78.
25. Bankole FA, Dako OF, Onalaja TA, Nwachukwu PS, Lateefat T. AI-driven fraud detection enhancing financial auditing efficiency and ensuring improved organizational governance integrity. Iconic Res Eng J. 2019;2(11):556-77.
26. Bidgoli AA. Simulation and optimization of primary oil and gas processing plant of FPSO operating in pre-salt oil field [doctoral dissertation]. São Paulo: Universidade de São Paulo; 2018.
27. Caicedo M, Barros J, Ordás B. Redefining agricultural residues as bioenergy feedstocks. Materials (Basel). 2016;9(8):635. doi:10.3390/ma9080635.
28. Carrasco JC, Lima FV. An optimization-based operability framework for process design and intensification of modular natural gas utilization systems. Comput Chem Eng. 2017;105:246-58. doi:10.1016/j.compchemeng.2017.02.006.
29. Chai KH, Yeo C. Overcoming energy efficiency barriers through systems approach—a conceptual framework. Energy Policy. 2012;46:460-72. doi:10.1016/j.enpol.2012.04.012.
30. Clark JH, Luque R, Matharu AS. Green chemistry, biofuels, and biorefinery. Annu Rev Chem Biomol Eng. 2012;3:183-207. doi:10.1146/annurev-chembioeng-062011-081014.
31. Cowie AL, Orr BJ, Sanchez VMC, Chasek P, Crossman ND, Erlewein A, *et al*. Land in balance: the scientific conceptual framework for Land Degradation Neutrality. Environ Sci Policy. 2018;79:25-35. doi:10.1016/j.envsci.2017.10.011.
32. Dako OF, Okafor CM, Farounbi BO, Onyelucheya OP. Detecting financial statement irregularities: hybrid Benford–outlier–process-mining anomaly detection architecture. IRE J. 2019;3(5):312-27.
33. Didi PU, Abass OS, Balogun O. A multi-tier marketing framework for renewable infrastructure adoption in emerging economies. RE J. 2019;3(4):337-45.
34. Erigha ED, Obuse E, Ayanbode N, Cadet E, Etim ED. Machine learning-driven user behavior analytics for insider threat detection. IRE J. 2019;2(11):535-44.
35. Evans-Uzosike IO, Okatta CG. Strategic human resource management: trends, theories, and practical implications. Iconic Res Eng J. 2019;3(4):264-70.

36. Fahd S, Fiorentino G, Mellino S, Ulgiati S. Cropping bioenergy and biomaterials in marginal land: the added value of the biorefinery concept. Energy. 2012;37(1):79-93. doi:10.1016/j.energy.2011.08.032.
37. Farounbi BO, Akinola AS, Adesanya OS, Okafor CM. Automated payroll compliance assurance: linking withholding algorithms to financial statement reliability. IRE J. 2018;1(7):341-57.
38. Gimelli A, Sannino R. A multi-variable multi-objective methodology for experimental data and thermodynamic analysis validation: an application to micro gas turbines. Appl Therm Eng. 2018;134:501-12. doi:10.1016/j.applthermaleng.2018.02.025.
39. Hamilton MS. Energy policy analysis: a conceptual framework. Abingdon: Routledge; 2014.
40. Hanachi H, Liu J, Banerjee A, Chen Y. A framework with nonlinear system model and nonparametric noise for gas turbine degradation state estimation. Meas Sci Technol. 2015;26(6):065604. doi:10.1088/0957-0233/26/6/065604.
41. Hendricks ES, Gray JS. pyCycle: a tool for efficient optimization of gas turbine engine cycles. Aerospace. 2019;6(8):87. doi:10.3390/aerospace6080087.
42. Hungbo AQ, Adeyemi C. Community-based training model for practical nurses in maternal and child health clinics. IRE J. 2019;2(8):217-35.
43. Hungbo AQ, Adeyemi C. Laboratory safety and diagnostic reliability framework for resource-constrained blood bank operations. IRE J. 2019;3(4):295-318.
44. Ibrahim TK, Basrawi F, Awad OI, Abdullah AN, Najafi G, Mamat R, *et al*. Thermal performance of gas turbine power plant based on exergy analysis. Appl Therm Eng. 2017;115:977-85. doi:10.1016/j.applthermaleng.2016.12.129.
45. Kamau EN. Energy efficiency comparison between 2.1 GHz and 28 GHz based communication networks [master's thesis]. Tampere: Tampere University of Technology; 2018.
46. Kyprianidis KG. On gas turbine conceptual design [doctoral dissertation]. Cranfield: Cranfield University; 2019.
47. Kyprianidis KG, Sethi V, Ogaji SOT, Pilidis P, Singh R, Kalfas AI. Uncertainty in gas turbine thermo-fluid modelling and its impact on performance calculations and emissions predictions at aircraft system level. Proc Inst Mech Eng G J Aerosp Eng. 2012;226(2):163-81. doi:10.1177/0954410011403845.
48. Lai KH, Lun VY, Wong CW, Cheng TCE. Green shipping practices in the shipping industry: conceptualization, adoption, and implications. Resour Conserv Recycl. 2011;55(6):631-8. doi:10.1016/j.resconrec.2010.12.004.
49. Larsson E, Åslund J, Frisk E, Eriksson L. Gas turbine modeling for diagnosis and control. J Eng Gas Turbines Power. 2014;136(7):071601. doi:10.1115/1.4026638.
50. Lee SY, Sankaran R, Chew KW, Tan CH, Krishnamoorthy R, Chu DT, *et al*. Waste to bioenergy: a review on the recent conversion technologies. BMC Energy. 2019;1:1-22. doi:10.1186/s42500-019-0003-7.
51. Li J, Zhang G, Ying Y. Gas turbine gas path fault diagnosis based on adaptive nonlinear steady-state thermodynamic model. Int J Perform Eng. 2018;14(4):751-9.
52. Lu H, Ma G, Azimi M, Fu L. Application of supergravity technology in a TEG dehydration process for offshore platforms. Processes. 2019;7(1):43. doi:10.3390/pr7010043.
53. Majoumerd MM, Somehsaraei HN, Assadi M, Breuhaus P. Micro gas turbine configurations with carbon capture—performance assessment using a validated thermodynamic model. Appl Therm Eng. 2014;73(1):172-84. doi:10.1016/j.applthermaleng.2014.07.044.
54. Menon V, Rao M. Trends in bioconversion of lignocellulose: biofuels, platform chemicals & biorefinery concept. Prog Energy Combust Sci. 2012;38(4):522-50. doi:10.1016/j.pecs.2012.02.002.
55. Mohan SV, Dahiya S, Amulya K, Katakojwala R, Vanitha TK. Can circular bioeconomy be fueled by waste biorefineries—a closer look. Bioresour Technol Rep. 2019;7:100277. doi:10.1016/j.biteb.2019.100277.
56. Moser BR. Camelina (Camelina sativa L.) oil as a biofuels feedstock: golden opportunity or false hope? Lipid Technol. 2010;22(12):270-3. doi:10.1002/lite.201000068.
57. Naik SN, Goud VV, Rout PK, Dalai AK. Production of first and second generation biofuels: a comprehensive review. Renew Sustain Energy Rev. 2010;14(2):578-97. doi:10.1016/j.rser.2009.10.003.
58. Naylor RL, Higgins MM. The rise in global biodiesel production: implications for food security. Glob Food Sec. 2018;16:75-84. doi:10.1016/j.gfs.2017.10.004.
59. Nguyen TV. Modelling, analysis and optimisation of energy systems on offshore platforms [doctoral dissertation]. Lyngby: Technical University of Denmark; 2014.
60. Nwokediegwu ZS, Bankole AO, Okiye SE. Advancing interior and exterior construction design through large-scale 3D printing: a comprehensive review. IRE J. 2019;3(1):422-49.
61. O'Connell D, Haritos VS. Conceptual investment framework for biofuels and biorefineries research and development. Biofuels. 2010;1(1):201-16. doi:10.4155/bfs.09.16.
62. Oguntegbe EE, Farounbi BO, Okafor CM. Conceptual model for innovative debt structuring to enhance mid-market corporate growth stability. IRE J. 2019;2(12):451-63.
63. Oguntegbe EE, Farounbi BO, Okafor CM. Empirical review of risk-adjusted return metrics in private credit investment portfolios. IRE J. 2019;3(4):494-505.
64. Oguntegbe EE, Farounbi BO, Okafor CM. Framework for leveraging private debt financing to accelerate SME development and expansion. IRE J. 2019;2(10):540-54.
65. Onalaja TA, Nwachukwu PS, Bankole FA, Lateefat T. A dual-pressure model for healthcare finance: comparing United States and African strategies under inflationary stress. IRE J. 2019;3(6):261-76.
66. Ong YK, Bhatia S. The current status and perspectives of biofuel production via catalytic cracking of edible and non-edible oils. Energy. 2010;35(1):111-9. doi:10.1016/j.energy.2009.09.004.
67. Oni O, Adeshina YT, Iloeje KF, Olatunji OO. Artificial intelligence model fairness auditor for loan systems. J ID. 2018;8993:1162.
68. Osabuohien FO. Review of the environmental impact of polymer degradation. Commun Phys Sci. 2017;2(1).

69. Osabuohien FO. Green analytical methods for monitoring APIs and metabolites in Nigerian wastewater: a pilot environmental risk study. Commun Phys Sci. 2019;4(2):174-86.
70. Parks D, Pack D. Design concept for implementation of a novel subsea gas dehydration process for a gas/condensate well. J Pet Sci Eng. 2013;109:18-25. doi:10.1016/j.petrol.2013.07.006.
71. Saboohi Z, Ommi F, Akbari M. Multi-objective optimization approach toward conceptual design of gas turbine combustor. Appl Therm Eng. 2019;148:1210-23. doi:10.1016/j.applthermaleng.2018.11.103.
72. Sayyaadi H, Mehrabipour R. Efficiency enhancement of a gas turbine cycle using an optimized tubular recuperative heat exchanger. Energy. 2012;38(1):362-75. doi:10.1016/j.energy.2011.11.053.
73. Stokes CS, Simpson AR, Maier HR. The cost–greenhouse gas emission nexus for water distribution systems including the consideration of energy generating infrastructure: an integrated conceptual optimization framework and review of literature. Earth Perspect. 2014;1:9. doi:10.1186/s40322-014-0009-5.
74. Udie J, Bhattacharyya S, Ozawa-Meida L. A conceptual framework for vulnerability assessment of climate change impact on critical oil and gas infrastructure in the Niger Delta. Climate. 2018;6(1):11. doi:10.3390/cli6010011.
75. Umoren O, Didi PU, Balogun O, Abass OS, Akinrinoye OV. Linking macroeconomic analysis to consumer behavior modeling for strategic business planning in evolving market environments. IRE J. 2019;3(3):203-13.
76. Welker CM, Balasubramanian VK, Petti C, Rai KM, DeBolt S, Mendu V. Engineering plant biomass lignin content and composition for biofuels and bioproducts. Energies (Basel). 2015;8(8):7654-76. doi:10.3390/en8087654.
77. Whalen J, Xu CC, Shen F, Kumar A, Eklund M, Yan J. Sustainable biofuel production from forestry, agricultural and waste biomass feedstocks. Appl Energy. 2017;198:281-3. doi:10.1016/j.apenergy.2017.04.025.
78. Yee SK, Milanović JV, Hughes FM. Validated models for gas turbines based on thermodynamic relationships. IEEE Trans Power Syst. 2011;26(1):270-81. doi:10.1109/TPWRS.2010.2053735.